View Online   Export Citation   CrossMark

Fantastic barocalorics and where to find them F SCI

View Online   Export Citation   CrossMark

David Boldrin[a] iD

AFFILIATIONS

SUPA, School of Physics and Astronomy, University of Glasgow, Glasgow G12 8QQ, United Kingdom

[a]Author to whom correspondence should be addressed: david.boldrin@glasgow.ac.uk

ABSTRACT

Barocaloric materials have the potential to offer greener and more efficient alternatives to conventional refrigerants that exploit vapor compression for cooling and heating applications. The barocaloric effect, a temperature change in response to hydrostatic pressure, is widespread in materials; however, only in the last few years have giant and colossal barocaloric effects approaching those of commercial hydrocarbon refrigerants been discovered. These barocaloric effects are associated with large changes in the degrees of freedom within the material and can take various forms. Here, we discuss this variety and categorize barocaloric materials based on the degree of freedom that underpins the barocaloric effects. We use this framework to identify material families to explore for potential barocalorics.

I. INTRODUCTION

The demand for heating, ventilation, air conditioning, and refrigeration (HVACR) in residential and industrial settings is growing rapidly. For instance, the global energy demand from air conditioners is expected to triple by 2050, amounting to ten new units sold every second until that date.[1] Vapor-compression technologies using hydrocarbon refrigerants dominate this industry. Despite the banning of many hydrocarbon refrigerants due to their Global Warming Potential (GWP) and negative impact on the environment, those used today still have a significant GWP. The development of new hydrocarbon refrigerants with lower GWP typically involves increased safety risks, such as flammability, and therefore, a trade-off must be made between safety and environmental concerns.[2] While many non-vapor-compression technologies exist, using refrigerants with essentially zero GWP, their efficiency and cost are currently vastly inferior.[3] Therefore, the discovery of new technologies with lower GWP and even modest improvements in efficiency have the potential to significantly reduce the environmental impact resulting from the rapid expansion of the HVACR sector.

Caloric materials are one of the main non-vapor compression alternatives as they can be significantly more efficient with essentially zero GWP.[3,4] They utilize changes in entropy and temperature, i.e., caloric effects, associated with ferroic transitions.[5] The best known of these are magneto-, elasto-, and electrocalorics, which use magnetic, stress, or electric fields to drive the transition, respectively. All these families display large caloric effects, making them promising refrigerants, and prototype devices have been developed for each.[6] However, barriers remain to commercialization, such as the cost of permanent magnets for magnetocalorics and the fatigue experienced by electro- and elasto-caloric materials during the several million cycles expected for a residential AC unit.

Barocalorics (BCs) are the least developed family of caloric materials. Analogous to vapor-compression refrigeration, temperature changes are driven by pressurization of the BC material [see Fig. 1(a)]. Compared to other calorics, they are less prone to fatigue and do not require expensive components to operate.[7] Until recently, they have not been considered competitive due to the large pressures required and, therefore, the small effects achievable in a realistic device. However, the giant ($\Delta S > 10$ J $K^{-1} kg^{-1}$) and colossal ($\Delta S > 100$ J $K^{-1} kg^{-1}$) BC effects (BCEs) discovered recently are the largest of any caloric material family[8,9] and can be achieved at relatively small pressures (<1 kbar). This has spurred interest in barocalorics as a real alternative to vapor-compression technologies, making them competitive with other caloric materials and technologies, as discussed in several excellent reviews.[4–7,10–13]

In this Perspective, we concentrate on reviewing the ever-growing number of BC materials that display giant and colossal effects. We classify the materials based on their underpinning physical mechanism and collate some of their key properties related to both their BCE and their application. We then look forward to which materials and mechanisms may lead to further advances in the field.

II. STATE-OF-THE-ART BAROCALORICS

Barocaloric effects are caused by changes in entropy within a material in response to hydrostatic pressure. If pressure is applied adiabatically to a barocaloric material, a temperature change results,
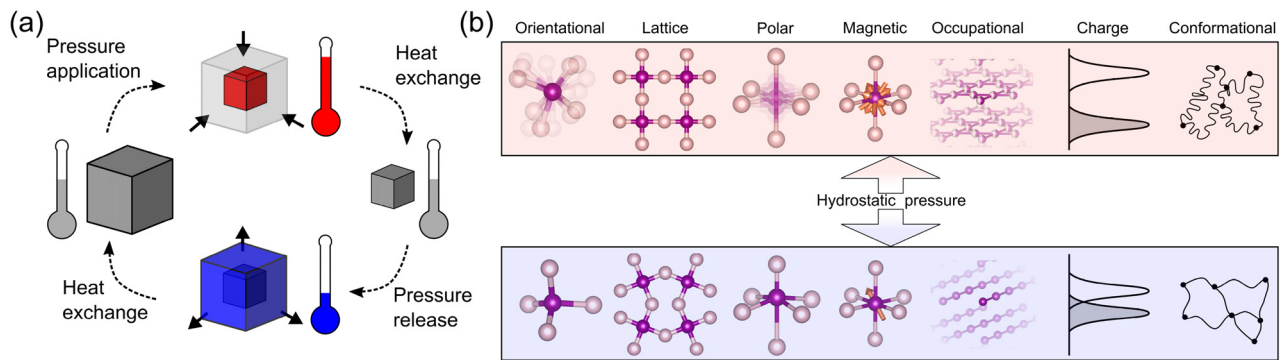
FIG. 1. (a) Schematic of a refrigeration cycle involving a material that possesses a conventional barocaloric effect. Inverse barocaloric effects are also found in some materials, where the application of hydrostatic pressure decreases temperature. (b) Different degrees of freedom able to couple to the lattice volume and, therefore, give rise to BCEs. Hydrostatic pressure is used to drive the system between the high entropy (top) and low entropy (bottom) states, typically across a 1st-order (discontinuous) transition. Under adiabatic conditions, this leads to a change in temperature of the material.

which is the basis of their use as refrigerants. More generally, in caloric materials, large entropy changes are associated with significant changes in the degrees of freedom within a material, typically across a 1st-order phase transition. This degree of freedom must couple to a property that can be changed using an external stimulus or field. For example, in magneto- and electro-calorics, the degree of freedom must couple to the magnetization and electric polarization, respectively. In barocalorics, the degree of freedom must couple to the lattice volume. Various couplings have been shown to give rise to large BCEs, some of which are depicted in Fig. 1(b), meaning that a rich and varying library of barocaloric materials is available to explore.

In order to discuss the materials, it is important to introduce some key BC parameters. Perhaps most important is the transitional entropy change, ΔS, most easily measured using differential scanning calorimetry (DSC). In the absence of DSC data, it can be estimated from the transitional entropy change given by the Clausius–Clapeyron relation,

$$\Delta S = \Delta V \left(\frac{\mathrm{d}T_\mathrm{t}}{\mathrm{d}p} \right)^{-1}, \qquad (1)$$

where ΔV is the volume change, T_t is the transition temperature, and p is the hydrostatic pressure. From this, it is clear that a large volume change and small sensitivity of the transition to pressure $(\frac{\mathrm{d}T_\mathrm{t}}{\mathrm{d}p})$ are beneficial. However, it is important to note that any BCE would vanish when $\frac{\mathrm{d}T_\mathrm{t}}{\mathrm{d}p} = 0$ and a large shift of the transition temperature is necessary to achieve large BCEs. The adiabatic temperature change, ΔT, is also commonly reported and directly relevant to the BCE; however, measuring ΔT directly is challenging and unreliable. Two alternative methods are commonly employed: (i) calorimetric quasi-direct methods, which are probably the most reliable, and (ii) estimation from the isothermal entropy change via $\Delta T = \frac{T\Delta S}{C}$, where C is the heat capacity, which typically overestimates values. In addition to the key BC properties, the thermal hysteresis and thermal conductivity are also important to consider for applications. Thermal hysteresis is an important property as it defines the reversibility of the effects; if the hysteresis is large, higher pressures are required to achieve the same BCE reversibly. Thermal conductivity is important for the efficient exchange of heat between the solid-state caloric material and the heat transfer fluid,[14] e.g., in the "heat exchange" steps of Fig. 1(a).

In order to aid discussion of the variety of BC materials, we have classified them according to the dominant degree of freedom underpinning the BCE, although in some materials, multiple couplings are involved. Within each subsection, we use this framework to initially discuss known BC materials before discussing those with similar degrees of freedom, which suggests the presence of large BCEs. All materials discussed, along with their key physical properties, are listed in Table I. For some degrees of freedom, such as those in solid electrolytes, recent theoretical work has already predicted BCEs. For others, we have looked through the literature for materials with relevant properties, such as transitional volume and/or enthalpy changes, which may translate into a significant BCE.

A. Orientational freedom

The benchmark for barocalorics has recently been set by a family of materials known as plastic crystals. They contain large organic molecules whose centers of mass form a crystalline lattice, yet due to their spherical shape, they are free to reorient and, thus, have many orientational degrees of freedom. The materials undergo a 1st-order transition and concomitant colossal entropy changes of $\Delta S > 100\,\mathrm{J\,kg^{-1}\,K^{-1}}$, of similar magnitude to commercial hydrocarbon refrigerants, due to the freezing of these reorientations.[8,9] This discovery has rightly generated much interest in barocaloric materials and highlighted the promise of materials with large orientational degrees of freedom. Indeed, further experiments demonstrated colossal BCEs in a number of plastic crystals.[15] Those with fcc cubic symmetry, rather than bcc, have significantly lower thermal hysteresis such that the BCEs are partially reversible. However, the thermal hysteresis remains high even in fcc-based materials, meaning that larger pressures are required to reversibly drive the BCEs.

Prior to the discovery of BCEs in plastic crystals, hybrid organic-inorganic perovskites demonstrated the potential of materials with large orientational (and lattice) degrees of freedom as barocalorics. These materials have long been investigated for their multifunctional properties, perhaps most notably as photovoltaics.[16] Relevant to barocalorics, the flexibility of the organic-inorganic motif leads to a variety of different 1st-order structural phase transitions with large volume changes. The resulting entropy changes are giant, with low thermal hysteresis of the transition, and occur under very low pressure changes

TABLE I. Key physical and barocaloric properties of the materials discussed in the text. T_t is the transition temperature, $\frac{dT_t}{dp}$ is the sensitivity of the transition to pressure, and ΔH is the transitional enthalpy change. Δp is the applied pressure used to measure ΔS, the isothermal entropy change, and ΔT, the adiabatic temperature change. For the latter, the superscipts indicate data collected using direct (D), quasi-direct (QD), or indirect (I) methods. All values refer to the maximum at the given pressure, not the reversible value. If possible, data with $\Delta p = 1$ kbar are used. The peak of the transition is used to determine the thermal hysteresis, T_{hys}. κ is the thermal conductivity.

Material name	Material type	Degree of freedom	T_t (K)	$\frac{dT_t}{dp}$ (K kbar^{-1})	$\Delta V/V$ (%)	ΔH (J g^{-1})	Δp (kbar)	ΔS (J kg^{-1} K^{-1})	ΔT (K)	T_{hys} (K)	κ (W m^{-1} K^{-1})	References
NPG	Plastic crystal	Orientational	320	~10	4.9	...	1	410	12[QD]	25	0.12[74]	9 and 15
PG	Plastic crystal	Orientational	352	~9	...	170	1	500	10[QD]	12	...	15
NPA	Plastic crystal	Orientational	220	~15	...	44	1	250	15[QD]	33	...	15
[TPrA][Mn(dca)$_3$]	hybrid perovskite	Orientational	330	23	1.2	...	1	35	5[QD]	0.9	0.3[75]	17
[(CH$_3$)$_4$N]Mn[N$_3$]$_3$	hybrid perovskite	Orientational	305	12	1.5	...	0.9	80	...	7	...	19
(NH$_4$)$_3$MoO$_2$F$_4$	Ferroelastic	Orientational	270	9.3	...	...	1	25	5[QD]	0.5	...	20
C$_{60}$	Molecular crystal	Orientational	257	17	1.0	7	1	32	9.7[QD]	0.5	1[76]	21
Li$_2$B$_{12}$H$_{12}$	Solid electrolyte	Orientational/ occupational	475	...	...	...	1	70[a]	...	...	...	22
(Me$_3$NNH$_2$)$_2$[Co(CN)$_6$ Na(H$_2$O)]	Ferroelastic	Orientational	290	...	...	...	...	146[b]	...	...	...	23
[(CH$_3$)$_3$NCH$_2$Cl] [FeCl$_4$]	Ionic plastic crystal	Orientational	322	...	...	50	...	152[b]	...	...	...	24
[(CH$_3$)$_3$NOH]$_2$ [KFe(CN)$_6$] (TMC-1)	Ionic plastic crystal	Orientational	402	...	...	99	...	...	...	...	...	26
Ni$_{49.26}$Mn$_{36.08}$In$_{14.66}$	Shape memory alloy	Magnetic	293	1.8	...	...	1	11	...	...	5–13[77,78]	31
(MnNiSi)$_{1-x}$(FeCoGe)$_x$	Shape memory alloy	Magnetic	280–311	~−7	2.7	...	1	42	7[QD]	4–12	...	79
MnCoGeB$_{0.03}$	Shape memory alloy	Magnetic	292	−10	4.4	...	1	35	10[QD]	18	...	30
Fe$_{49}$Rh$_{51}$	Metamagnet	Magnetic	310	6.4	...	...	1	12	...	9	...	32
LaFe$_{11.33}$Co$_{0.47}$Si$_{1.2}$	Magnetocaloric	Magnetic	240	...	1.1	...	1	6	1.5[D]	...	...	28
Mn$_3$GaN	Frustrated antiferromagnet	Magnetic	293	−6.5	1.0	...	1	22	5[QD]	...	5 – 15[80]	33
Mn$_3$NiN	Frustrated antiferromagnet	Magnetic	262	−1.4	0.4	...	1	22	1.5[QD]	2[81]	...	34
[FeL$_2$][BF$_4$]$_2$	Spin crossover	Spin	260	12	2.6	...	0.43	68	4.5[QD]	4	...	35
Fe$_3$(bntrz)$_6$(tcnset)$_6$	Spin crossover	Spin	318	25	3.6	25	0.9	100	20[QD]	2	...	36
CrAs	Antiferromagnet	Magnetic	265	28	2.4	...	...	...	...	...	...	37
Ni$_{0.85}$Fe$_{0.15}$S	Itinerant metal	Charge	305	−7.5	1.4	...	1	52	10[QD]	11.5	5–12[42]	42
V$_{1-x}$(W, Cr)$_x$O$_2$	Transition metal oxide	Charge	280–400	...	...	...	...	100 − 150[b]	...	...	...	45
RCu$_3$Fe$_4$O$_{12}$	Transition metal oxide	Charge	250–360	...	...	...	...	60 − 70[b]	...	...	...	45
(NH$_4$)$_2$SO$_4$	Ferrielectric	Polar	219	~−5	0.5	...	1	60	8[ID]	3	0.82[82]	48
BaTiO$_3$	Ferroelectric	Polar	400	−5.6	0.1	...	1	1.5	...	1	...	47
Sc$_{1-x}$Ti$_x$F$_3$ (x = 0.85)	Open framework	Lattice	290	72	...	...	1	12[a]	...	...	...	49
ZIF-4(Co,Zn)	Zeolite	Lattice	293	...	19 [Co]	21 [Zn]	...	...	...	...	...	50 and 51
ZIF-8	Zeolite	Lattice	290	...	...	10	...	...	...	...	...	53
Ag$_3$[Co(CN)$_6$]	Framework material	Lattice	293	...	16	...	...	...	...	...	...	55

TABLE I. (Continued.)

Material name	Material type	Degree of freedom	T_t (K)	$\frac{dT_t}{dp}$ (K kbar^{-1})	$\Delta V/V$ (%)	ΔH (J g^{-1})	Δp (kbar)	ΔS (J kg^{-1} K^{-1})	ΔT (K)	T_{hys} (K)	κ (W m^{-1} K^{-1})	References
AgI	Solid electrolyte	Occupational	395	−13	5	...	1	60	10[QD]	24	0.2[83]	57
Li$_3$N	Solid electrolyte	Occupational	300[c]	...	...	...	10	25[a]	...	...	...	56
Cu$_2$Se	Solid electrolyte/thermoelectric	Occupational/charge	400–700[c]	...	...	...	10	17.5[a]	...	...	...	59
PVDF-TrFE-CTFE	Polymer	Conformational/polar	335	~25	...	...	0.8	50	10[ID]	...	...	63
GVG(VPGVG)	Elastin-like polypeptide	Conformational	298	...	...	...	...	~200[b]	...	...	...	66
R134a	Commercial refrigerant	Translational	295	...	...	...	0.01	610	...	...	...	84

[a] Barocaloric entropy change calculated for the given pressure.
[b] Transitional entropy change at ambient pressure.
[c] Operating temperatures, T_t, not associated with a phase transition.

($<$0.1 kbar).[17,18] Their operating temperatures are often far from room temperature; however, their chemical flexibility allows tuning of the transition temperature.[19]

A material family traditionally explored for ferroelectric properties is ferroelastics that contain fluoride or oxyfluoride MO_xF_{6-x} distorted octahedral groups. A number of these crystallize in centrosymmetric space groups, which means that they cannot be ferroelectric; however, some of these non-polar materials display large BCEs due to the orientational ordering of the (oxy)fluoride groups.[20] The magnitude of the BCE is similar to the organic-inorganic perovskites, although significantly larger pressures are required, and both also share chemical flexibility (where M takes many transition metal elements), meaning that there is scope for tuning their BC properties. A recent discovery in this class of materials is fullerite, C_{60}, which displays large, reversible BCEs across a wide temperature range spanning room temperature.[21] The rotations of the nearly spherical C_{60} molecules undergo a partial freezing at $T \sim 257\,K$ with a remarkably small thermal hysteresis, giving rise to a giant BCE with pressures as low as 0.5 kbar.

The entropy changes associated with the BCEs of materials with many orientational degrees of freedom approach those of commercial fluid hydrocarbon refrigerants (see R134a in Table I for comparison).[9] However, certain obstacles to applications remain. The thermal hysteresis of plastic crystals is particularly large and is the main drawback for these colossal BC materials as it increases the pressures required in a device. For all these organic-based materials, the low thermal conductivity is also detrimental within a device.

Looking to the future, theory and preliminary experiments have already predicted two promising materials based on their orientational degree of freedom: lithium borohydrides[22] and a new inorganic-organic hybrid ferroelastic.[23] The former are a new barocaloric material family that undergoes an order-disorder transition ($T > 450\,K$) that involves entropic contributions from both Li^+ diffusion and reorientation of the $(BH)_{12}^{-2}$ icosahedra, with colossal entropy changes predicted. The latter is similar to the ferroelastic barocaloric materials already discussed, but involves the cleavage of weak bonds between organic cations and inorganic anions. For this material, the ambient pressure entropy change measured across the transition ($T \sim 290\,K$) is colossal; however, no pressure-dependent studies have yet been performed.

Ionic plastic crystals contain inorganic and organic ionic moieties with large orientational disorder, similar to the purely organic molecular plastic crystals already discussed. Given their similarity and the fact that they also undergo strongly 1st-order transitions with large latent heat and volume changes, one would expect them to possess BCEs.[24–26] Moreover, inclusion of transition metals adds functionality that may facilitate multicaloric control and tends to increase the melting temperature compared to purely organic materials (molecular plastic crystals have melting temperatures close to room temperature). Indeed, it is this additional functionality that means they have been heavily studied as solid state electrolytes.[27] Thus, a number of different materials are known and could immediately be explored as barocalorics.[24]

B. Magnetic freedom

Given the relative maturity of the field of magnetocalorics and the fact that strong magnetovolume correlations commonly coexist with magnetocaloric effects, it is no surprise that these systems have also been investigated for their BCEs. For instance, the alloy families La-Fe-Si-Co,[28] MnCoGe$_{1-x}$(In,B)$_x$,[29,30] Ni-Mn-In,[31] and FeRh[32] all

undergo strongly 1st-order transitions between low magnetization and ferromagnetic states, leading to a magnetocaloric effect with a concurrent change in the volume, leading to a BCE. Given that this caloric mechanism has been well studied, we will not discuss it in depth here; however, their BC properties are listed in Table I. These materials typically possess a giant BCE at room temperature although the thermal hysteresis is also large thermal hysteresis.

In fact, coupling between magnetism and the lattice volume can arise in a number of ways and in materials with low magnetization that are not applicable to magnetocalorics. The antiperovskite family Mn_3XN (X = Ga[33] and Ni[34]) hosts non-collinear antiferromagnetic structures that are strongly coupled to the lattice volume. A large change in the volume occurs at the 1st-order transition between paramagnetic (PM) and antiferromagnetic (AFM) states, and moreover, the giant BCE at this transition is enhanced by frustrated interactions between both local and itinerant electronic moments.

While dissimilar to the order-disorder magnetic transitions discussed, in spin-crossover (SCO) compounds, e.g., $[FeL_2][BF_4]_2$, the volume change between different spin configurations of crystal-field split d-orbitals underpins the giant BCEs.[35] The giant BCEs can be driven by pressures as small as 0.3 kbar due to the extreme sensitivity of the crossover transition to pressure. Very recent results on $Fe_3(bntrz)_6(tcnset)_6$ reveal some of the largest adiabatic temperature changes ($\sim$20 K for 0.9 kbar) of any caloric material, which are almost fully reversible due to the small hysteresis (4 K).[36] No values of the thermal conductivity could be found for this material family; however, one might expect them to be similar to the hybrid organic-inorganic perovskites.

For the inorganic magnetic systems, while mass normalized values of the barocaloric entropy changes are an order of magnitude smaller than those of, e.g., plastic crystals, the volume normalized values are of similar magnitude because of their larger physical density. The relevance of this remains to be seen; however, it is linked to another benefit of these materials: their typically large thermal conductivity (see Table I). Finally, for all these magnetic materials, as with the hybrid organic-inorganic systems, their chemical flexibility provides opportunities to tune key parameters (transition temperature and thermal hysteresis) synthetically, e.g., by doping, alloying, or ligand choice.

New magnetic or spin-based BCE materials are likely to be found in two categories: antiferromagnetic materials and SCO compounds. Of the antiferromagnetic materials, only the Mn_3XN antiperovskites with X = Ga and Ni have been studied for their BCEs.[33,34] Aside from this family, several other antiferromagnets exist with strong coupling between the magnetism and the volume. Unfortunately, this coupling typically results from magnetic frustration, which suppresses the magnetic transition to temperatures well below room temperature. We identified two materials that warrant measurements of their BCE. First is CrAs, which is isostructural to the MnP-related magnetocalorics. It undergoes a 1st-order PM-AFM transition at $T = 265$ K with a 2.4% volume change.[37] Doping with S elevates the transition temperature and it would be worth investigating how this impacts the 1st-order transition.[38] Second is YMn_2, which undergoes a PM-AFM transition with a giant volume change of 5%.[39] The transition temperature is too low for room temperature caloric applications ($T \sim 100$ K[39]) but it may be possible to adjust this by doping while maintaining the volume change. Further examples of antiferromagenetic compounds relevant

to barocalorics may come from the active field of antiferromagnetic spintronics,[40] where coupling between the lattice and the magnetic structure is typically a prerequisite.

For SCO compounds, a great wealth of chemical flexibility exists. It is worth noting here that the majority of entropic contributions at the SCO transition can originate from the vibrational entropy associated with the ligands, rather than that originating from spin freedom in the low spin and high spin states.[41] This suggests that the ligand choice may have dramatic effects on the BCEs, and therefore, plentiful opportunities remain to investigate further SCO materials for yet larger BCEs.

C. Charge freedom

In transition metal compounds, phase transitions can involve coupling between several degrees of freedom associated with the electronic structure, e.g., spin (magnetism), charge (metal-insulator transitions), and orbital (orbital ordering). The transition metal sulfide $Ni_{1-x}Fe_xS$ undergoes a 1st-order metal-insulator transition (MIT) between a PM metal and an AFM nonmetal and, therefore, involves both charge and magnetic degrees of freedom. The resulting giant BCE is the largest of any of the metallic magnets under 1 kbar; however, the thermal hysteresis requires significantly larger pressures to obtain reversible effects.[42] Although the material is antiferromagnetic, electronic structure calculations show that a significant restructuring of the electronic density of states occurs at the MIT, and therefore, the latter is the dominant contribution to the BCE.

The MIT of $Ni_{1-x}Fe_xS$ is the only one to be studied for its BCE to our knowledge. In general, MITs have long interested solid-state physicists, from both a theoretical and practical perspective, and have, therefore, been studied in a number of different materials. They are generally 1st-order transitions, involving significant crystal structure changes, and can be found in a number of transition metal compounds. Vanadium oxides are one of the archetypal material families showing MITs. For example, VO_2 displays a strongly 1st-order MIT at 340 K, and indeed, this transition has been studied for thermal storage applications due to entropy changes of $\sim$150 J kg^{-1} K^{-1}.[43] Significant work has been invested in this material in order to tune the MIT, such as controlling the temperature with W-doping[43] and hysteresis,[44] which could be adapted for the purposes of tuning potential BCEs. Aside from VO_2, certain other materials are of interest. $RCu_3Fe_4O_{12}$ (R = rare-earth metal) perovskites have recently been investigated as thermal storage materials due to the large changes in charge degrees of freedom at the MIT.[45] These materials display an entropy change of $\sim$50 J kg^{-1} K^{-1} associated with either charge transfer or charge disproportionation, and by changing the R-cation the MIT temperature can be tuned with little effect on the transitional entropy change.[45] Finally, analogous to the hybrid organic-inorganic perovskites with large orientational degrees of freedom, organic-based materials with MITs may provide additional entropic contributions due to ordering of the organic molecules.[46]

D. Lattice and polar freedom

Several of the degrees of freedom depicted in Fig. 1 could be considered as lattice freedoms, for instance, orientational and occupational. Here, we discuss materials where the entropic contributions to

07 July 2023 10:07:40

the BCE are associated with cooperative tilting, rotations, or displacements of the lattice rather than those of molecular subunits or sublattices. Of these, only polar materials have thus far been studied experimentally for their BCEs and these are ferroelectric $BaTiO_3$[47] and ferrielectric ammonium sulfate, $(NH_4)_2SO_4$.[48] In both materials, the BCEs are caused by volume changes occurring at symmetry breaking transitions, with the former involving a traditional polar displacive transition and the latter a unique ionic ordering. The properties of $(NH_4)_2SO_4$ are of particular note due to the large entropy changes achievable at small pressures. Unfortunately, its transition temperature is well below room temperature, making it unrealistic as a BC. Instead, these results highlight the possibility of achieving impressive BCEs in polar materials and, by extension, in materials with significant lattice freedom.

Theoretical studies of the open-framework material $Sc_{1-x}Ti_xF_3$ have already provided evidence of the potential BCEs in materials with lattice degrees of freedom.[49] This material is a member of the metal trifluoride family, MF_3, which are isostructural to ABO_3 perovskites with a vacant A-site. These open-framework materials often display abnormal thermal expansion properties due to cooperative tilting and rotations of the crystal structure. In $Sc_{0.15}Ti_{0.85}F_3$, a 1st-order transition at room temperature, involving antiferrodistortive rotations of the MF_6 octahedra, is predicted to lead to a giant BCE. This occurs over a very broad temperature range ($\sim$50 K for 1 kbar) due to an enormous sensitivity of the transition temperature to pressure and additional significant volume changes far from the transition. Although, the hybrid organic-inorganic materials discussed in Sec. II A may also be considered an open framework, confirming the BCE in $Sc_{1-x}Ti_xF_3$ would encourage the exploration of inorganic open-framework materials.

Beyond theoretical studies, we can look for indirect evidence of BCE behavior in other flexible lattice material families. Some of the most studied are zeolites, which can also be considered a type of open-framework material. Several zeolites undergo 'breathing transitions' between open pore (op) and closed pore (cp) structures under temperature and/or hydrostatic pressure changes, particularly within the zeolitic imidazolate framework (ZIF) subfamily. The magnitude of the volume change between op and cp structures is typically $\sim$20%, although the transitions are often irreversible. ZIF-4(Co) presents an excellent BC candidate, as the transition involves a 19% volume change, can be driven with 0.5 kbar, and is fully reversible.[50] Calorimetric studies of the same transition in ZIF-4(Zn) driven by temperature ($T_t \sim 140$ K) give an enthalpy change of $\Delta H \sim 21$ J g^{-1},[51] suggesting that a similar magnitude latent heat can be expected when driving the transition of ZIF-4(Co) with pressure at room temperature.

Zeolites offer an alternative mechanism to BCEs. The intrusion and extrusion of solvents, such as water, causes condensation of the solvent in the pores of zeolites and acts like a genuine 1st-order phase transition.[52] For instance, extrusion and intrusion of water into ZIF-8 leads to large enthalpy changes (> 10 J g^{-1}) and this transition can be reversibly driven at room temperature with a pressure of 0.3 kbar.[53] These properties mean that zeolite ZIF-8 has been studied as a potential energy storage material. If these translate into good BCEs, via either mechanism, the range and chemical flexibility of zeolites mean that many materials are available to study.

We finally discuss the BC potential of flexible lattice materials that show extreme compressibility. Cyanide-based framework materials, for instance Prussian Blue, $Fe_4[Fe(CN)_6]_3$, and its analogues, have been studied for a long time due to their anomalous thermal expansion properties related to the flexibility of their lattice. Extreme compressibility is a consequence of this flexibility in some of these materials, such as $LnFe(CN)_6$[54] and $Ag_3[Co(CN)_6]$.[55] In both these materials, volume compression occurs at a rate of $\sim$2% per kbar pressure. This value is comparable to the transitional volume change in many of the BC materials discussed and an order of magnitude larger than the superionic regime of Li_3N discussed in Sec. II E ($\sim$0.1% per kbar).[56] As in the latter, these changes are not associated with a transition and so should not be hysteretic. For $Ag_3[Co(CN)_6]$, pressure also induces a 1st-order structural phase transition at $p = 1.9$ kbar, which involves a giant volume change of 16%.[55] This transition further enhances its potential as a BCE although no calorimetry data could be found on it.

E. Occupational freedom

Occupational freedom refers to the disorder of ionic sublattices within materials, typically found in solid electrolytes and leading to BCEs quite different from the materials discussed. In AgI, a 1st-order order-disorder transition of the Ag sublattice occurs; above the transition, the Ag cations are disordered across a number of sites, and below the transition, these order.[57] This transition leads to significant changes in the ionic conductivity and lattice volume and, consequently, giant BCEs over a very broad temperature range. Of particular note are the adiabatic temperature changes, $\Delta T = 10$ K, which are similar to those of plastic crystals. However, drawbacks include the following: (i) the large thermal hysteresis of the transition results in a significant increase in the required pressure to reversibly drive the transition and (ii) a transition temperature that is far from room temperature. Nonetheless, the results demonstrate how theoretical exploration, which had previously predicted large mechanocaloric effects in solid electrolytes,[58] can play a crucial role in discovering novel barocaloric materials.

Theoretical studies have already provided predictions of significant BCEs in two solid electrolytes. In Li_3N, it is noted that a giant BCE can be induced far from a phase transition.[56] In many of the order-disorder transitions discussed (magnetic, orientational, polar,...), the order parameter saturates in the ordered phase, meaning that away from a transition, no appreciable entropy change can be induced by pressure. However, in Li_3N, the ionic conductivity is strongly dependent on pressure far from the transition to ionic conduction. The promising aspect of this is that the effects are non-hysteretic, due to the lack of a transition; however, the downside is that relatively large pressures are required ($\Delta S/\Delta p \sim 3$ J kg^{-1} K^{-1} kbar^{-1}).[56] Another theoretical study of the thermoelectric solid electrolyte Cu_2Se showed similar properties, which also highlights the potential for thermoelectric materials.[59]

F. Conformational freedom

We finish this section by discussing BCEs that arise from conformational degrees of freedom. Various forms of rubber have shown promise as BC materials due to the large entropy changes caused by rearrangements of elastomer chains and associated changes in conformational freedom, under hydrostatic pressure. For instance, experiments on vulcanized natural,[60] PDMS,[61] and nitrile[62] rubbers have demonstrated giant entropy changes upon application of pressure

07 July 2023 10:07:40

(although for these experiments, this was not applied in a truly hydrostatic way). Moreover, it appears that BCEs are not limited to rubber elastomers but can also be found in other polymers. The ferroelectric polymer PVDF-TrFE-CTFE (trifluoroethylene-chlorotrifluoroethylene) displays giant BCEs associated with both conformational and polar degrees of freedom.[63] Away from the ferroelectric phase transition, giant BCEs of $\sim$20 J kg^{-1} K^{-1} are achievable across a broad temperature range under 1 kbar, while at the ferroelectric phase transition ($T \sim 320$ K), ΔS peaks at $\sim$50 J kg^{-1} K^{-1} at the same applied pressure. In all these materials, the changes in conformational freedom are not associated with a phase transition and, therefore, should, in theory, not be hysteretic (although nitrile rubber does display a small hysteresis[62]). The wide variety of known polymers and elastomers mean that many materials are available to study; however, their typically small thermal conductivity may prove problematic.

The wide variety of elastomers and polymers mean that there is a large source of potential BC materials to be explored in this family. However, the BCE of these materials is perhaps of more interest as it suggests that many other materials with conformational degrees of freedom may possess significant BCEs. An obvious analogy is the conformational freedom of proteins. Indeed, denaturing of proteins is known to be strongly dependent on pressures and can be reversibly driven using relatively low pressures on the order of kbar.[64] An interesting candidate would be the mammalian protein elastin, which is present in connective tissues in animals, due to its remarkable elasticity. Unlike other proteins, it undergoes a unique thermally induced transition close to room temperature, termed 'inverse temperature transition' (ITT), where the volume collapses upon heating due to the expulsion of water molecules within the protein.[65] This ITT is present in many elastin-like polypeptides. Calorimetric studies of GVG(VPGVG) show a large latent heat at the ITT, with $\Delta S \sim 200$ J kg^{-1} K^{-1}, which can also be driven reversibly with pressure.[66]

III. MATERIALS OPTIMIZATION

The focus of the article is on materials discovery; however, we will briefly discuss potential improvements to known barocalorics. The development of devices has been instigated by the recent discoveries discussed in Sec. II, and therefore, it would be beneficial to tailor the known barocalorics in tandem with device engineering. Given the colossal BCE values already observed, it is perhaps more important to focus on improving key secondary parameters related to the workings of a device, such as thermal conductivity and thermal hysteresis. Thermal conductivity, which tends to remain fairly constant within material families, can potentially be improved in organic-based materials via the use of composite materials, e.g., by incorporating inclusions of metallic barocalorics in a composite matrix. The inclusions could be tuned such that their transition coincides with that of the organic and, moreover, could be chosen such that they have the opposite entropy change (i.e., conventional or inverse BCE). An alternative approach is to improve the thermal conductivity of the heat transfer fluid, e.g., by including high thermal conductivity particles, modeling of which shows improved device efficiency.[67]

Thermal hysteresis can vary considerably within material families, and, as such, there is considerable scope to improve this property intrinsically, either through synthetic methods or by the discovery of new materials. For instance, different plastic crystals show vastly different thermal hysteresis. In inorganic or metallic systems, thermal

hysteresis can potentially be optimized synthetically or by doping and/or alloying. For instance, quaternary $Mn_3(Zn,In)N$ shows remarkably small hysteresis despite large values in some ternary systems, e.g., Mn_3GaN.[68] Methods for tailoring hysteresis in magnetic systems may also be developed from the recent discovery of a non-hysteretic 1st-order transition in Eu_2In.[69,70] A rich source of literature dealing with thermal hysteresis is available from the wider caloric field from which innovative methods to minimize could be adapted to barocalorics, such as by using multicaloric cycles where more than one stimulus is used (e.g., magnetic field and hydrostatic pressure).[71–73]

IV. CONCLUSIONS

The discovery of colossal barocaloric effects, larger than any other caloric effect and comparable to conventional refrigerants, has rightly attracted much attention and excitement. Despite these recent advances, it is worth remembering that the study of barocalorics is still at an early stage and many obstacles remain to commercialization. In addition to the ongoing efforts of those studying caloric materials, collaboration with broader sections of the scientific community is now required to overcome these challenges and realize the full potential of barocalorics. Yet, its infancy as a field also suggests that the ever-growing variety of materials that show BCEs are not expected to slow down and there is clear potential for further improvements. We hope that this article stimulates the study of several novel barocaloric materials and the exploration of different mechanisms that may give rise to barocaloric effects.

DATA AVAILABILITY

Data sharing is not applicable to this article as no new data were created or analyzed in this study.

REFERENCES

[1]International Energy Agency (IEA), *The Future of Cooling Opportunities for Energy- Efficient Air Conditioning* (IEA, 2018).

[2]M. O. McLinden, C. J. Seeton, and A. Pearson, "New refrigerants and system configurations for vapor-compression refrigeration," Science **370**, 791–796 (2020).

[3]W. Goetzler, R. Shandross, J. Young, O. Petritchenko, D. Ringo, and S. McClive, *Energy Savings Potential and RD&D Opportunities for Commercial Building HVAC Systems* (U.S. Department of Energy, 2017), p. 172.

[4]X. Moya and N. D. Mathur, "Caloric materials for cooling and heating," Science **370**, 797–803 (2020).

[5]X. Moya, S. Kar-Narayan, and N. D. Mathur, "Caloric materials near ferroic phase transitions," Nat. Mater. **13**, 439–450 (2014).

[6]A. Greco, C. Aprea, A. Maiorino, and C. Masselli, "A review of the state of the art of solid-state caloric cooling processes at room-temperature before 2019," Int. J. Refrigeration **106**, 66–88 (2019).

[7]L. Mañosa and A. Planes, "Materials with giant mechanocaloric effects: Cooling by strength," Adv. Mater. **29**, 1603607 (2017).

[8]B. Li, Y. Kawakita, S. Ohira-Kawamura, T. Sugahara, H. Wang, J. Wang, Y. Chen, S. I. Kawaguchi, S. Kawaguchi, K. Ohara, K. Li, D. Yu, R. Mole, T. Hattori, T. Kikuchi, S.-I. Yano, Z. Zhang, Z. Zhang, W. Ren, S. Lin, O. Sakata, K. Nakajima, and Z. Zhang, "Colossal barocaloric effects in plastic crystals," Nature **567**, 506–510 (2019).

07 July 2023 10:07:40

9 P. Lloveras, A. Aznar, M. Barrio, P. Negrier, C. Popescu, A. Planes, L. Mañosa, E. Stern-Taulats, A. Avramenko, N. D. Mathur, X. Moya, and J.-L. Tamarit, "Colossal barocaloric effects near room temperature in plastic crystals of neopentylglycol," Nat. Commun. 10, 1803 (2019).

10 L. Mañosa and A. Planes, "Solid-state cooling by stress: A perspective," Appl. Phys. Lett. 116, 050501 (2020).

11 C. Cazorla, "Novel mechanocaloric materials for solid-state cooling applications," Appl. Phys. Rev. 6, 041316 (2019).

12 J. Zhang, Y. Xu, S. An, Y. Sun, X. Li, and Y. Li, "Giant mechanocaloric materials for solid-state cooling," Chin. Phys. B 29, 076202 (2020).

13 S. Crossley, N. D. Mathur, and X. Moya, "New developments in caloric materials for cooling applications," AIP Adv. 5, 067153 (2015).

14 A. Kitanovski, U. Plaznik, U. Tomc, and A. Poredoš, "Present and future caloric refrigeration and heat-pump technologies," Int. J. Refrigeration 57, 288–298 (2015).

15 A. Aznar, P. Lloveras, M. Barrio, P. Negrier, A. Planes, L. Mañosa, N. D. Mathur, X. Moya, and J. L. Tamarit, "Reversible and irreversible colossal barocaloric effects in plastic crystals," J. Mater. Chem. A 8, 639–647 (2020).

16 G. Hodes, "Perovskite-Based Solar Cells," Science 342, 317–319 (2013).

17 J. M. Bermúdez-García, M. Sánchez-Andújar, S. Castro-García, J. López-Beceiro, R. Artiaga, and M. A. Señarís-Rodríguez, "Giant barocaloric effect in the ferroic organic-inorganic hybrid [TPrA] [Mn(dca) 3] perovskite under easily accessible pressures," Nat. Commun. 8, 15715 (2017).

18 J. M. Bermúdez-García, S. Yáñez-Vilar, A. García-Fernández, M. Sánchez-Andújar, S. Castro-García, J. López-Beceiro, R. Artiaga, M. Dilshad, X. Moya, and M. A. Señarís-Rodríguez, "Giant barocaloric tunability in [(CH3CH2CH2)4N]Cd [N(CN)2]3 hybrid perovskite," J. Mater. Chem. C 6, 9867–9874 (2018).

19 J. Salgado-Beceiro, A. Nonato, R. X. Silva, A. García-Fernández, M. Sánchez-Andújar, S. Castro-García, E. Stern-Taulats, M. A. Señarís-Rodríguez, X. Moya, and J. M. Bermúdez-García, "Near-room-temperature reversible giant barocaloric effects in [(CH3)4N]Mn [N3]3 hybrid perovskite," Mater. Adv. 1, 3167–3170 (2020).

20 M. V. Gorev, E. V. Bogdanov, I. N. Flerov, A. G. Kocharova, and N. M. Laptash, "Investigation of thermal expansion, phase diagrams, and barocaloric effect in the (NH4)2WO2F4 and (NH4)2MoO2F4 oxyfluorides," Phys. Solid State 52, 167–175 (2010).

21 J. Li, D. Dunstan, X. Lou, A. Planes, L. Mañosa, M. Barrio, J. L. Tamarit, and P. Lloveras, "Reversible barocaloric effects over a large temperature span in fullerite C60," J. Mater. Chem. A 8, 20354–20362 (2020).

22 K. Sau, T. Ikeshoji, S. Takagi, S. I. Orimo, D. Errandonea, D. Chu, and C. Cazorla, "Colossal barocaloric effects in the complex hydride Li2B12H12," preprint arXiv:2008.07102 (2020).

23 W. J. Xu, Y. Zeng, W. Yuan, W. X. Zhang, and X. M. Chen, "A large room-temperature entropy change in a new hybrid ferroelastic with an unconventional bond-switching mechanism," Chem. Commun. 56, 10054–10057 (2020).

24 D. Li, X. M. Zhao, H. X. Zhao, L. S. Long, and L. S. Zheng, "Coexistence of magnetic-optic triple switching and thermal energy storage in a multifunctional plastic crystal of trimethylchloromethyl ammonium tetrachloroferrate(III)," Inorg. Chem. 58, 655–662 (2019).

25 J. Salgado-Beceiro, J. M. Bermúdez-García, A. L. Llamas-Saiz, S. Castro-García, M. A. Señarís-Rodríguez, F. Rivadulla, and M. Sánchez-Andújar, "Multifunctional properties and multi-energy storage in the [(CH3)3S] [FeCl4] plastic crystal," J. Mater. Chem. C 8, 13686–13694 (2020).

26 W. J. Xu, P. F. Li, Y. Y. Tang, W. X. Zhang, R. G. Xiong, and X. M. Chen, "A molecular perovskite with switchable coordination bonds for high-temperature multiaxial ferroelectrics," J. Am. Chem. Soc. 139, 6369–6375 (2017).

27 J. M. Pringle, P. C. Howlett, D. R. MacFarlane, and M. Forsyth, "Organic ionic plastic crystals: Recent advances," J. Mater. Chem. 20, 2056–2062 (2010).

28 L. Mañosa, D. González-Alonso, A. Planes, M. Barrio, J.-L. Tamarit, I. S. Titov, M. Acet, A. Bhattacharyya, and S. Majumdar, "Inverse barocaloric effect in the giant magnetocaloric La–Fe–Si–Co compound," Nat. Commun. 2, 595 (2011).

29 R.-R. Wu, L.-F. Bao, F.-X. Hu, H. Wu, Q.-Z. Huang, J. Wang, X.-L. Dong, G.-N. Li, J.-R. Sun, F.-R. Shen, T.-Y. Zhao, X.-Q. Zheng, L.-C. Wang, Y. Liu, W.-L. Zuo, Y.-Y. Zhao, M. Zhang, X.-C. Wang, C.-Q. Jin, G.-H. Rao, X.-F. Han, and B.-G. Shen, "Giant barocaloric effect in hexagonal Ni2 In-type Mn-Co-Ge-In compounds around room temperature," Sci. Rep. 5, 18027 (2015).

30 A. Aznar, P. Lloveras, J. Y. Kim, E. Stern-Taulats, M. Barrio, J. L. Tamarit, C. F. Sánchez-Valdés, J. L. Sánchez Llamazares, N. D. Mathur, and X. Moya, "Giant and reversible inverse barocaloric effects near room temperature in ferromagnetic MnCoGeB0.03," Adv. Mater. 31, 1903577–1903576 (2019).

31 L. Mañosa, D. González-Alonso, A. Planes, E. Bonnot, M. Barrio, J.-L. Tamarit, S. Aksoy, and M. Acet, "Giant solid-state barocaloric effect in the Ni–Mn–In magnetic shape-memory alloy," Nat. Mater. 9, 478–481 (2010).

32 E. Stern-Taulats, A. Planes, P. Lloveras, M. Barrio, J. L. Tamarit, S. Pramanick, S. Majumdar, C. Frontera, and L. Mañosa, "Barocaloric and magnetocaloric effects in Fe49Rh51," Phys. Rev. B 89, 214105 (2014).

33 D. Matsunami, A. Fujita, K. Takenaka, and M. Kano, "Giant barocaloric effect enhanced by the frustration of the antiferromagnetic phase in Mn3GaN," Nat. Mater. 14, 73–78 (2015).

34 D. Boldrin, E. Mendive-Tapia, J. Zemen, J. B. Staunton, T. Hansen, A. Aznar, J.-L. Tamarit, M. Barrio, P. Lloveras, J. Kim, X. Moya, and L. F. Cohen, "Multisite exchange-enhanced barocaloric response in Mn3NiN," Phys. Rev. X 8, 041035 (2018).

35 S. P. Vallone, A. N. Tantillo, A. M. dos Santos, J. J. Molaison, R. Kulmaczewski, A. Chapoy, P. Ahmadi, M. A. Halcrow, and K. G. Sandeman, "Giant barocaloric effect at the spin crossover transition of a molecular crystal," Adv. Mater. 31, 1807334–1807337 (2019).

36 M. Romanini, Y. Wang, K. Gürpinar, G. Ornelas, P. Lloveras, Y. Zhang, W. Zheng, M. Barrio, A. Aznar, B. Emre, O. Atakol, C. Popescu, H. Zhang, Y. Long, L. Balicas, J. L. Tamarit, A. Planes, M. Shatruk, and L. Manosa, "Giant and reversible barocaloric effect in trinuclear spin-crossover complex Fe 3 (bntrz) 6 (tcnset) 6," Adv. Mater. 33, 2008076 (2021).

37 T. Suzuki and H. Ido, "3d metal-substitution effects on magnetic and crystallographic properties of CrAs," J. Appl. Phys. 69, 4624–4626 (1991).

38 T. Suzuki and H. Ido, "Magnetic and crystallographic properties of CrAs1xSx(0x<1)," J. Appl. Phys. 79, 5224 (1996).

39 H. Nakamura, H. Wada, K. Yoshimura, M. Shiga, Y. Nakamura, J. Sakurai, and Y. Komura, "Effect of chemical pressure on the magnetism of YMn2: Magnetic properties of Y1-xScxMn2 and Y1-xLaxMn2," J. Phys. F: Met. Phys. 18, 981–991 (1988).

40 V. Baltz, A. Manchon, M. Tsoi, T. Moriyama, T. Ono, and Y. Tserkovnyak, "Antiferromagnetic spintronics," Rev. Mod. Phys. 90, 015005 (2018).

41 P. Gütlich and H. A. Goodwin, "Spin crossover—An overall perspective," Top. Curr. Chem. 233, 1–47 (2004).

42 J. Lin, P. Tong, X. Zhang, Z. Wang, Z. Zhang, B. Li, G. Zhong, J. Chen, Y. Wu, H. Lu, L. He, B. Bai, L. Ling, W. Song, Z. Zhang, and Y. Sun, "Giant room-temperature barocaloric effect at the electronic phase transition in Ni1-xFexS," Mater. Horiz. 7, 2690–2695 (2020).

43 S. Niitaka, H. Takagi, and M. Miyano, Japan patent JP2010163510A (July 2010).

44 S. Chen, J. Liu, L. Wang, H. Luo, and Y. Gao, "Unraveling mechanism on reducing thermal hysteresis width of VO2 by Ti doping: A joint experimental and theoretical study," J. Phys. Chem. C 118, 18398–18944 (2014).

45 T. Uchimura and I. Yamada, "A robust thermal-energy-storage property quadruple perovskite oxides †," Chem. Commun. 56, 5500–5503 (2020).

46 K. Saito, S. Ikeuchi, A. Ota, H. Yamochi, and G. Saito, "Entropic evidence for cooperation of multiple instabilities upon a metal–insulator transition in (EDO-TTF)2PF6," Chem. Phys. Lett. 401, 76–79 (2005).

47 E. Stern-Taulats, P. Lloveras, M. Barrio, E. Defay, M. Egilmez, A. Planes, J. L. Tamarit, L. Mañosa, N. D. Mathur, and X. Moya, "Inverse barocaloric effects in ferroelectric BaTiO3 ceramics," APL Mater. 4, 091102 (2016).

48 P. Lloveras, E. Stern-Taulats, M. Barrio, J.-L. Tamarit, S. Crossley, W. Li, V. Pomjakushin, A. Planes, L. Mañosa, N. D. Mathur, and X. Moya, "Giant barocaloric effects at low pressure in ferrielectric ammonium sulphate," Nat. Commun. 6, 8801 (2015).

49 A. Corrales-Salazar, R. T. Brierley, P. B. Littlewood, and G. G. Guzmán-Verri, "Landau theory and giant room-temperature barocaloric effect in M F3 metal trifluorides," Phys. Rev. Mater. 1, 053601 (2017).

50 S. Henke, M. T. Wharmby, G. Kieslich, I. Hante, A. Schneemann, Y. Wu, D. Daisenberger, and A. K. Cheetham, "Pore closure in zeolitic imidazolate frameworks under mechanical pressure," Chem. Sci. 9, 1654–1660 (2018).

51 M. T. Wharmby, S. Henke, T. D. Bennett, S. R. Bajpe, I. Schwedler, S. P. Thompson, F. Gozzo, P. Simoncic, C. Mellot-Draznieks, H. Tao, Y. Yue, and

07 July 2023 10:07:40

A. K. Cheetham, "Extreme flexibility in a zeolitic imidazolate framework: Porous to dense phase transition in desolvated ZIF-4," Angew. Chem. **127**, 6547–6551 (2015).

[52] G. Fraux, F. X. Coudert, A. Boutin, and A. H. Fuchs, "Forced intrusion of water and aqueous solutions in microporous materials: From fundamental thermodynamics to energy storage devices," Chem. Soc. Rev. **46**, 7421–7437 (2017).

[53] Y. Grosu, V. Eroshenko, J. M. Nedelec, and J. P. Grolier, "A new working mode for molecular springs: Water intrusion induced by cooling and associated isobaric heat capacity change of a {ZIF-8 + water} system," Phys. Chem. Chem. Phys. **17**, 1572–1574 (2015).

[54] S. G. Duyker, V. K. Peterson, G. J. Kearley, A. J. Studer, and C. J. Kepert, "Extreme compressibility in LnFe(CN)$_6$ coordination framework materials via molecular gears and torsion springs," Nat. Chem. **8**, 270–275 (2016).

[55] A. L. Goodwin, D. A. Keen, and M. G. Tucker, "Large negative linear compressibility of Ag$_3$ [Co(CN)$_6$]," Proc. Natl. Acad. Sci. U. S. A. **105**, 18708–18713 (2008).

[56] A. K. Sagotra, D. Chu, and C. Cazorla, "Room-temperature mechanocaloric effects in lithium-based superionic materials," Nat. Commun. **9**, 3337 (2018).

[57] A. Aznar, P. Lloveras, M. Romanini, M. Barrio, J.-L. Tamarit, C. Cazorla, D. Errandonea, N. D. Mathur, A. Planes, X. Moya, and L. Mañosa, "Giant barocaloric effects over a wide temperature range in superionic conductor AgI," Nat. Commun. **8**, 1851 (2017).

[58] C. Cazorla and D. Errandonea, "Giant mechanocaloric effects in fluorite-structured superionic materials," Nano Lett. **16**, 3124–3129 (2016).

[59] J. Min, A. K. Sagotra, and C. Cazorla, "Prediction of large barocaloric effects in thermoelectric superionic materials," Phys. Rev. Mater. **4**, 015403 (2020).

[60] E. O. Usuda, N. M. Bom, and A. M. Carvalho, "Large barocaloric effects at low pressures in natural rubber," Eur. Polym. J. **92**, 287–293 (2017).

[61] A. M. G. Carvalho, W. Imamura, E. O. Usuda, and N. M. Bom, "Giant room-temperature barocaloric effects in PDMS rubber at low pressures," Eur. Polym. J. **99**, 212–221 (2018).

[62] E. O. Usuda, W. Imamura, N. M. Bom, L. S. Paixão, and A. M. Carvalho, "Giant reversible barocaloric effects in Nitrile Butadiene Rubber around room temperature," ACS Appl. Polym. Mater. **1**, 1991–1997 (2018).

[63] S. Patel, A. Chauhan, R. Vaish, and P. Thomas, "Elastocaloric and barocaloric effects in polyvinylidene di-fluoride-based polymers," Appl. Phys. Lett. **108**, 072903 (2016).

[64] R. Ravindra and R. Winter, "On the temperature—Pressure free-energy landscape of proteins," ChemPhysChem **4**, 359–365 (2003).

[65] S. Perticaroli, G. Ehlers, N. Jalarvo, J. Katsaras, and J. D. Nickels, "Elasticity and inverse temperature transition in elastin," J. Phys. Chem. Lett. **6**, 4018–4025 (2015).

[66] C. Nicolini, R. Ravindra, B. Ludolph, and R. Winter, "Characterization of the temperature- and pressure-induced inverse and reentrant transition of the minimum elastin-like polypeptide GVG(VPGVG) by DSC, PPC, CD, and FT-IR spectroscopy," Biophys. J. **86**, 1385–1392 (2004).

[67] C. Aprea, A. Greco, A. Maiorino, and C. Masselli, "Enhancing the heat transfer in an active barocaloric cooling system using ethylene-glycol based nanofluids as secondary medium," Energies **12**, 2902 (2019).

[68] D. Boldrin, E. Mendive-Tapia, J. Zemen, J. Staunton, A. M. Gomes, L. Ghivelder, J. Halpin, A. Gibbs, A. Aznar, J.-L. Tamarit, P. Lloveras, X. Moya, and L. F. Cohen, "Barocaloric Properties of Quaternary Mn$_3$(Zn,In)N for Room Temperature Refrigeration Applications" (unpublished).

[69] F. Guillou, A. K. Pathak, D. Paudyal, Y. Mudryk, F. Wilhelm, A. Rogalev, and V. K. Pecharsky, "Non-hysteretic first-order phase transition with large latent heat and giant low-field magnetocaloric effect," Nat. Commun. **9**, 2925 (2018).

[70] E. Mendive-Tapia, D. Paudyal, L. Petit, and J. B. Staunton, "First-order ferromagnetic transitions of lanthanide local moments in divalent compounds: An itinerant electron positive feedback mechanism and Fermi surface topological change," Phys. Rev. B **101**, 174437 (2020).

[71] Y. Liu, L. C. Phillips, R. Mattana, M. Bibes, A. Barthélémy, and B. Dkhil, "Large reversible caloric effect in FeRh thin films via a dual-stimulus multicaloric cycle," Nat. Commun. **7**, 11614 (2016).

[72] T. Gottschall, A. Gràcia-Condal, M. Fries, A. Taubel, L. Pfeuffer, L. Mañosa, A. Planes, K. P. Skokov, and O. Gutfleisch, "A multicaloric cooling cycle that exploits thermal hysteresis," Nat. Mater. **17**, 929–934 (2018).

[73] A. Gracia-Condal, T. Gottschall, L. Pfeuffer, O. Gutfleisch, A. Planes, and L. Manosa, "Multicaloric effects in metamagnetic Heusler Ni-Mn-In under uniaxial stress and magnetic," Appl. Phys. Rev. **7**, 041406 (2020).

[74] S. Akbulut, Y. Ocak, K. Keşlioğlu, and N. Maraşli, "Thermal conductivities of solid and liquid phases for neopentylglycol, aminomethylpropanediol and their binary alloy," J. Phys. Chem. Solids **70**, 72–78 (2009).

[75] B. K. Shaw, A. R. Hughes, M. Ducamp, D. A. Keen, F. X. Coudert, F. Blanc, and T. D. Bennett, "Hybrid inorganic-organic perovskite glasses," chemRxiv:11956599.v1 (2020).

[76] V. B. Efimov, L. P. Mezhov-Deglin, and R. K. Nikolaev, "Thermal conductivity of crystalline fullerite C60 in the simple cubic phase," JETP Lett. **65**, 687–693 (1997).

[77] Q. Zheng, G. Zhu, Z. Diao, D. Banerjee, and D. G. Cahill, "High contrast thermal conductivity change in Ni–Mn–In Heusler alloys near room temperature," Adv. Eng. Mater. **21**, 1801342 (2019).

[78] B. Zhang, X. X. Zhang, S. Y. Yu, J. L. Chen, Z. X. Cao, and G. H. Wu, "Giant magnetothermal conductivity in the Ni–Mn–In ferromagnetic shape memory alloys," Appl. Phys. Lett. **91**, 012510 (2007).

[79] P. Lloveras, T. Samanta, M. Barrio, I. Dubenko, N. Ali, J. L. Tamarit, and S. Stadler, "Giant reversible barocaloric response of (MnNiSi)1- x(FeCoGe)x (x = 0.39, 0.40, 0.41)," APL Mater. **7**, 061106 (2019).

[80] J. C. Lin, B. S. Wang, P. Tong, W. J. Lu, L. Zhang, X. B. Zhu, Z. R. Yang, W. H. Song, J. M. Dai, and Y. P. Sun, "AlN [sub x]Mn [sub 3]: A possible high-temperature soft magnetic material and strongly correlated system," Appl. Phys. Lett. **98**, 092507 (2011).

[81] M. Wu, C. Wang, Y. Sun, L. Chu, J. Yan, D. Chen, Q. Huang, and J. W. Lynn, "Magnetic structure and lattice contraction in Mn3NiN," J. Appl. Phys. **114**, 123902 (2013).

[82] T. K. Song, S.-M. Lee, Y. S. Yu, and S.-I. Kwun, "Dielectric and thermal studies on the high temperature phases of (NH$_4$)$_2$SO$_4$," Ferroelectrics **159**, 215–220 (1994).

[83] M. C. Goetz and J. A. Cowen, "The thermal conductivity of silver iodide," Solid State Commun. **41**, 293–295 (1982).

[84] M. O. McLinden, *ASHRAE Handbook* (ASHRAE, Atlanta, 2009).

07 July 2023 10:07:40